

Gaussian versus Superposition States: Potentiality to store quantum information under dissipative dynamics

L. A. M. Souza¹*, M. C. Nemes¹, M. França Santos¹ and J. G. Peixoto de Faria²

¹*Departamento de Física, Instituto de Ciências Exatas, Universidade Federal de Minas Gerais, CP 702, CEP 30161-970, Belo Horizonte, Minas Gerais, Brasil;*

²*Departamento Acadêmico de Disciplinas Básicas, Centro Federal de Educação Tecnológica de Minas Gerais, 30510-000, Belo Horizonte, MG, Brasil.*

The dissipative dynamics of Gaussian squeezed states (GSS) and coherent superposition states (CSS) are analytically obtained and compared. Time scales for sustaining different quantum properties such as squeezing, negativity of the Wigner function or photon number distribution are calculated. Some of these characteristic times also depend on initial conditions. For example, in the particular case of squeezing, we find that while the squeezing of CSS is only visible for small enough values of the field intensity, in GSS it is independent of this quantity, which may be experimentally advantageous. The asymptotic dynamics however is quite similar as revealed by the time evolution of the fidelity between states of the two classes.

PACS numbers: 03.65.-w, 03.65.Yz, 03.67.-a

I. INTRODUCTION

The recent rapid development of quantum information theory has largely stimulated research on nonclassical states of light. A particularly promising approach consists in processing quantum information with continuous variables [1], where the information is encoded into two conjugate quadratures of the quantized mode of the optical field. Natural candidates for these applications are Gaussian squeezed states (for a review of experiments with squeezed light see [2]) and superpositions of two coherent states [3]. Both classes of quantum states present different quantum properties (see [4, 5, 6, 7, 8, 9, 10, 11, 12, 13, 14, 15, 16] and references therein) such as squeezing, oscillations in the photon number distribution and sub-Poissonian statistics [17].

When comparing the utility of Gaussian squeezed states (GSS) and superpositions of coherent states (CSS) for quantum information processing and storage, one is compelled to consider practical points such as how easy it is to produce each one of them. However, when dealing with information storage it is also important, to take into account the system's behavior under dissipative dynamics. For example, although GSS are easier to produce than CSS, it is conceivable that the quantum properties present in both classes of states possess different characteristic time scales, which may suggest CSS as better candidates for quantum information processing. Such analysis can help deciding which state to choose and how to experimentally optimize the manipulation of these quantum properties.

Several recent experiments have shown that quantum features of light are usually sensitive to dissipation. Squeezing, oscillations in photon number distribution

and interference effects are dramatically reduced when the physical system is coupled to a macroscopic environment. There is a vast literature on both cases (see [18] and references therein for a review). The question we address in this contribution is: how fast do the two classes of initial states (CSS or GSS) lose their potentiality to exhibit each one of the quantum properties they have in common and/or others?

Whether a quantum state can be described classically cannot be decided on the measurement of a single observable, i.e. a classical description may explain some behavior and fail to explain another. We therefore analytically derive, according to the model presented, characteristic time scales for different quantum properties in both classes of states: GSS and CSS. In particular, we show that although these classes of states share some quantum features as e.g. squeezing and oscillations in photon number distribution, their time scales are both quantitatively and qualitatively different. For superposition states, there is a well known time scale related to the time it takes for the corresponding Wigner functions to become completely positive. This is called decoherence time. It means that, in this time scale, interference effects become unobservable. We show that the time scale for observing squeezing effects or oscillations in photon number distribution is *smaller* than the decoherence time and this limitation is due to the dependence of these times on the intensity of the coherent fields. For GSS, however, the situation drastically changes. The characteristic times for the observation of the same properties are *independent* of the intensity, an effect obtained numerically in reference [19]. In this contribution, for the sake of comparison, we consider states of both classes with comparable characteristic times. This allows us to show that the dynamics leading to the asymptotic stationary state is very similar, so that all interesting physics is contained in the transient times. Moreover, for the GSS considered it is possible to obtain an upper limit on the initial thermal excitations so that quantum proper-

*e-mail: lamsouza@fisica.ufmg.br

ties may still be visible [20].

This work is divided as follows: we study some quantum properties of coherent superposition states (section II) and of displaced, squeezed, thermal states (section III). The quantum properties are, in both cases and respectively: squeezing and interference (subsections II A-III A), oscillations in photon number distribution (subsections II B-III B) and the von Neumann entropy (subsections II C-III C). Besides the qualitative comparisons made in the cited sections, in section IV we present an analytical expression for the fidelity between the superposition states and the GSS as a function of time. In section V we briefly summarize this work and present the conclusions.

II. SUPERPOSITION STATES: DISSIPATIVE DYNAMICS OF QUANTUM PROPERTIES

The class of initial states here considered can be written as pure superposition states of the form

$$|\psi\rangle = \frac{1}{N} \left(|\beta_0\rangle + e^{i\theta} |-\beta_0\rangle \right), \quad (1)$$

where

$$N = \sqrt{2(1 + e^{-2|\beta_0|^2} \cos \theta)} \quad (2)$$

and $|\beta_0\rangle$ stands for a coherent state. If $\theta = 0(\pi)$ we will have an even (odd) coherent superposition state (which we shall, from now on call even (odd) superposition states). These states can be produced both in cavity QED [21] and propagating pulses [22] and have been utilized mainly to study the effects of decoherence and quantum-classical transition.

The dissipative dynamics we have in mind is the one well known from quantum optics

$$\dot{\rho} = \mathcal{L}\rho, \quad (3)$$

with

$$\begin{aligned} \mathcal{L}\cdot = & -i\omega[a^\dagger a, \cdot] + k(\bar{n}_B + 1)(2a \cdot a^\dagger - a^\dagger a \cdot - \cdot a^\dagger a) \\ & + k \bar{n}_B(2a^\dagger \cdot a - aa^\dagger \cdot - \cdot aa^\dagger), \end{aligned} \quad (4)$$

where ω is the angular frequency of the unitary evolution, \bar{n}_B is the mean number of excitations in the environment and k is the system-environment coupling constant. In this work we use units such that $\hbar = 1$.

The solution for the zero temperature case (also well known) is given by

$$\begin{aligned} \rho_A(t) = & \frac{1}{N^2} \left\{ |\beta(t)\rangle \langle \beta(t)| + |-\beta(t)\rangle \langle -\beta(t)| + f(\beta_0, t) \times \right. \\ & \left. \times (e^{i\theta} |\beta(t)\rangle \langle -\beta(t)| + e^{-i\theta} |-\beta(t)\rangle \langle \beta(t)|) \right\}, \end{aligned} \quad (5)$$

where N is given in equation (2),

$$f(\beta_0, t) = e^{-2(|\beta_0|^2 - |\beta(t)|^2)} \quad (6)$$

and

$$\beta(t) = \beta_0 e^{-(i\omega + k)t}. \quad (7)$$

Note that the stationary solution is a pure Gaussian state

$$\rho_A(t \rightarrow \infty) = |0\rangle \langle 0|, \quad (8)$$

where $|0\rangle$ is such that $a|0\rangle = 0$. In this section we will only consider zero temperature for simplicity.

The density operator (5) has the following eigenvectors [23]

$$|e(t)\rangle = \frac{1}{N_e(t)} [|\beta(t)\rangle + |-\beta(t)\rangle], \quad (9)$$

$$|o(t)\rangle = \frac{1}{N_o(t)} [|\beta(t)\rangle - |-\beta(t)\rangle]$$

whose eigenvalues are given by

$$p_e(t) = \frac{1}{N^2} (1 + e^{-2|\beta(t)|^2}) (1 + e^{-2(|\beta_0|^2 - |\beta(t)|^2)} \cos \theta), \quad (10)$$

$$p_o(t) = \frac{1}{N^2} (1 - e^{-2|\beta(t)|^2}) (1 - e^{-2(|\beta_0|^2 - |\beta(t)|^2)} \cos \theta),$$

where

$$\begin{aligned} N_e(t) &= \sqrt{2(1 + e^{-2|\beta(t)|^2})} \\ N_o(t) &= \sqrt{2(1 - e^{-2|\beta(t)|^2})}. \end{aligned} \quad (11)$$

The subscripts e and o stand for even and odd superpositions states respectively.

A. Interference and Squeezing

The potentiality of superposition states to produce interference is encoded in the negative parts of their Wigner functions. In the present case, the time evolution of the Wigner function for states of the form (1) is given by

$$\begin{aligned} W(\lambda, \lambda^*, t) = & \frac{4}{N^2} \left\{ e^{-2|\beta(t)|^2 - 2|\lambda|^2} \cosh \left[4|\beta(t)|^2 \Re \left(\frac{\lambda}{\beta(t)} \right) \right] \right. \\ & \left. + f(\beta_0, t) e^{-2|\lambda|^2} \cos \left[\theta - 2|\beta(t)|^2 \Im \left(\frac{\lambda}{\beta(t)} \right) \right] \right\}. \end{aligned} \quad (12)$$

The above expression has been obtained using the relation $W(\lambda, \lambda^*) = 2 \text{tr}[\rho_A D(\lambda) (-1)^{\hat{n}} D^{-1}(\lambda)]$, where $D(\lambda)$ is the displacement operator, $(-1)^{\hat{n}}$ is the parity operator, $\lambda = \sqrt{\frac{\omega}{2}}(x + ip)$ and the symbols \Re , \Im stand for real and imaginary parts respectively.

Some results for the Wigner function (WF) at time zero ($t = 0$) of the even and odd coherent superposition

states are shown in figures (1) - (4), for different values of β_0 .

The negative part of the WF for the same value of β_0 is systematically larger for odd superposition states. However it disappears simultaneously in the well known decoherence time $\tau = (4|\beta_0|^2 k)^{-1}$. When this time is reached, there are no quantum effects which remain, neither squeezing nor oscillating photon number distribution, as we shall show shortly. These phenomena however possess different time scales than that of decoherence. In figure (1) it is clear (at least qualitatively) that the WF of a even CSS, with small values of β_0 , is quasi-Gaussian, the crucial difference is that it shows interference (the negative parts). When we increase the value of β_0 , the negative parts of the even CSS are clear. The odd CSS always has a negative value of Wigner function, particularly in the point $x = p = 0$.

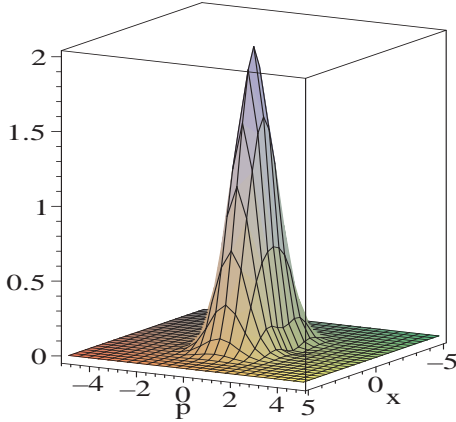


FIG. 1: Wigner function for the even superposition state ($\theta = 0$). Parameters: $\beta_0 = 0.8$, $\omega = 1$, $k = 0.1$, $t = 0$.

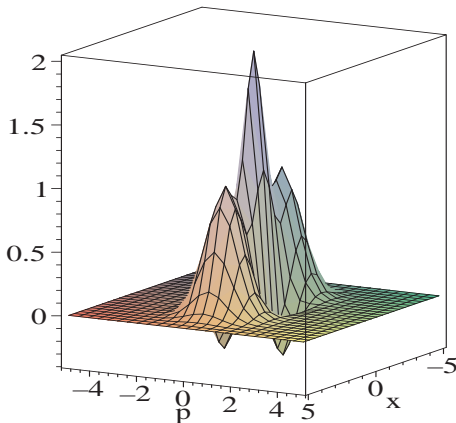


FIG. 2: Wigner function for the even superposition state ($\theta = 0$). Parameters: $\beta_0 = 1.5$, $\omega = 1$, $k = 0.1$, $t = 0$.

An interesting physically appealing way to understand the dynamics of the WF for the even and odd superposition states is as follows: in figure (5) we plot the

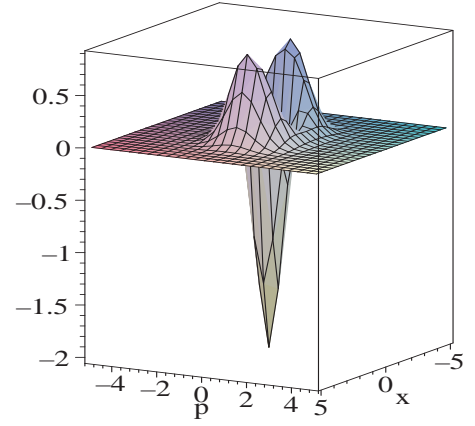


FIG. 3: Wigner function for the even superposition state ($\theta = \pi$). Parameters: $\beta_0 = 0.8$, $\omega = 1$, $k = 0.1$, $t = 0$.

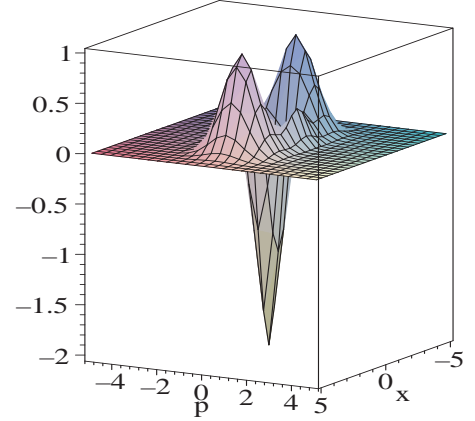


FIG. 4: Wigner function for the even superposition state ($\theta = \pi$). Parameters: $\beta_0 = 1.5$, $\omega = 1$, $k = 0.1$, $t = 0$.

fidelity of each state with the vacuum state (to be asymptotically reached) as a function of time. The fidelity $F(\rho_A, |0\rangle\langle 0|) = \sqrt{\langle 0|\rho_A|0\rangle}$ is given by

$$F^2(\rho_A, |0\rangle\langle 0|) = \frac{2e^{-|\beta(t)|^2}}{N^2} \left(1 + f(\beta_0, t) \cos \theta \right), \quad (13)$$

where $f(\beta_0, t)$ is given by (6), N is the normalization (2) and $\beta(t)$ is given by (7).

Initially the odd superposition state does not contain the vacuum in its structure. However, since this state is a fixed point of the dynamics (its pointer state), it needs to be populated. As can be gathered from the figure, the vacuum state is rapidly populated. As for the even superposition state, if $\beta_0 \lesssim 1.14$ (for our choice of parameters), the initial probability of finding the vacuum in that state is always larger than 50%. There comes the difference with the odd superposition state. While the latter rapidly populates the vacuum state, the even superposition state starts by populating other states maintaining the vacuum population practically unchanged. Af-

ter these initial different transient time both states have similar dynamics, evolving both to the asymptotic state $|0\rangle\langle 0|$.

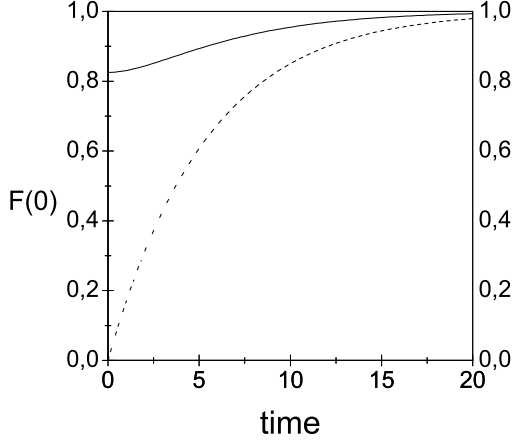


FIG. 5: Fidelity between the vacuum state and even ($\theta = 0$, solid line) and odd ($\theta = \pi$, dash line) superposition states. Parameters: $\beta_0 = 0.8$, $\omega = 1$, $k = 0.1$. The time scale is: time $= \omega t$.

Next, we show that the characteristic time of squeezing effects is shorter than that for interference effects. The tool we use here to investigate squeezing in the quadratures is the determinant of the covariance matrix

$$D(t) = \text{Det} \begin{pmatrix} \sigma_{pp} & \sigma_{qp} \\ \sigma_{qp} & \sigma_{qq} \end{pmatrix}, \quad (14)$$

where $\sigma_{qq} = \langle x^2 \rangle - \langle x \rangle^2$, $\sigma_{pp} = \langle p^2 \rangle - \langle p \rangle^2$ and $\sigma_{qp} \cdot \sigma_{pq} = \frac{1}{4} \langle xp + px \rangle^2$. For CSS, we have

$$\begin{aligned} \langle x^2 \rangle &= \frac{1}{2\omega} \left\{ 1 + \beta^2 + \beta^{*2} + \frac{4|\beta|^2}{N^2} [1 - \cos(\theta)e^{-2|\beta_0|^2}] \right\} \\ \langle p^2 \rangle &= -\frac{\omega}{2} \left\{ -1 + \beta^2 + \beta^{*2} - \frac{4|\beta|^2}{N^2} [1 - \cos(\theta)e^{-2|\beta_0|^2}] \right\} \\ \langle xp + px \rangle &= -i(\beta^2 - \beta^{*2}). \end{aligned}$$

since the non-diagonal terms precisely cancel the rapid oscillations due to the free field frequency. Note that, for this case, $\langle x^2 \rangle = \sigma_{qq}$ and $\langle p^2 \rangle = \sigma_{pp}$.

As can be noted from the expressions for $\langle x^2 \rangle$ and $\langle p^2 \rangle$ (showed explicitly in [9]) the odd superposition state will never exhibit squeezing. However, the even superposition is always squeezed.

In figures (6) and (7) we show the determinant of the covariance matrix for the even and odd superposition states. As can be seen from the figure, the squeezing

of the even superposition state (“filtered” by the determinant) increases, reaching a maximum value and then following the dissipative dynamics which will take it to the vacuum state. The time of the maximum value of the determinant (and of the squeezing “visibility”) depends on β_0 as follows

$$t_c^S = -\frac{1}{2k} \ln \left[\frac{\sinh(2|\beta_0|^2)}{4|\beta_0|^2 \cos \theta} \right], \quad (15)$$

and the effect is only visible for small enough values of β_0 , i. e., only if

$$0 < \frac{\sinh(2|\beta_0|^2)}{4|\beta_0|^2 \cos \theta} < 1. \quad (16)$$

For the even states

$$0 \leq t_c^S \leq \tau, \quad (17)$$

where τ is the decoherence time (note that for the odd CSS the characteristic time does not have physical interpretation, it acquires imaginary values). For large values of β_0 the squeezed quadrature is essentially constant, and the determinant of the covariance matrix is very similar for both the even and odd superposition states. We remark that the visibility of the effect is a consequence of two factors: the initial conditions must obey the above inequality and the characteristic times must be experimentally “available”.

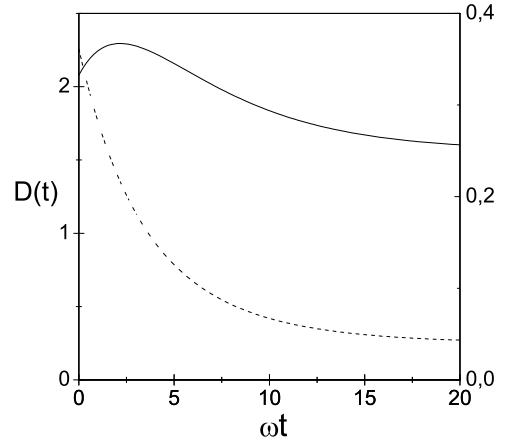


FIG. 6: Time evolution of the determinant of the covariance matrix for the even superposition state (solid line, right scale) and for the odd superposition state (dash line, left scale). Parameters: $\beta_0 = 0.8$, $\omega = 1$, $k = 0.1$.

B. Oscillating photon distribution

The time evolution of the photon distribution for the even and odd superposition states for different values of β_0 is depicted in figures (8)-(11). The analytic expression for these curves is given by ($P_n = \langle n|\rho|n \rangle$)

$$P_n = e^{-|\beta(t)|^2} \frac{2|\beta(t)|^{2n}}{N^2 n!} [1 + (-1)^n f(\beta_0, t) \cos \theta]. \quad (18)$$

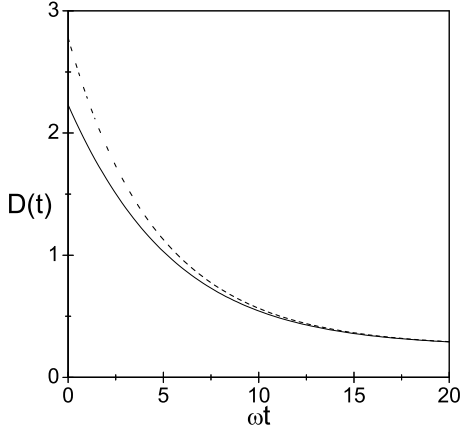


FIG. 7: Time evolution of the determinant of the covariance matrix for the even superposition state (solid line) and for the odd superposition state (dash line). Parameters: $\beta_0 = 1.5$, $\omega = 1$, $k = 0.1$.

Note that the dissipative dynamics will tend to destroy the initial parity of the states. The characteristic time is approximately the same as that for the squeezing of the even superposition state. The solid line is intended to guide the eye. Also, it is well known that while coherent states have Poissonian photon distribution, even (odd) superposition states have super(sub)-Poissonian distributions. This can be measured by the Mandel parameter Q defined as

$$Q = \frac{\langle (\Delta n)^2 \rangle - \langle n \rangle}{\langle n \rangle}. \quad (19)$$

Here, $\langle n \rangle$ and $\langle (\Delta n)^2 \rangle$ are the average and the variance of photon number in the field state, respectively. If the distribution is sub-Poissonian, i. e. $Q < 0$, the state is a quantum one. If $Q \geq 0$ however, no definite statement can be made. For example, in our case, the even CSS is “as quantum” as the odd one, despite presenting super-Poissonian statistics (just like “classical” light) [9], which evidences that in order to decide whether a state is quantum or not, most likely more than one pertinent observables should be measured. The exception to this case is the set of states that present negative Wigner function in which case a simple measurement of this negativity is enough to preclude any classical analog.

C. von Neumann entropy

Having obtained the eigenvalues of the density matrices of even and odd superposition states, it is a simple matter to calculate von Neumann’s entropy, which is depicted in figures (12)-(13) for different values of β_0 . The von Neumann entropy is given by

$$S[\rho] = -\text{tr}(\rho \ln \rho) \quad (20)$$

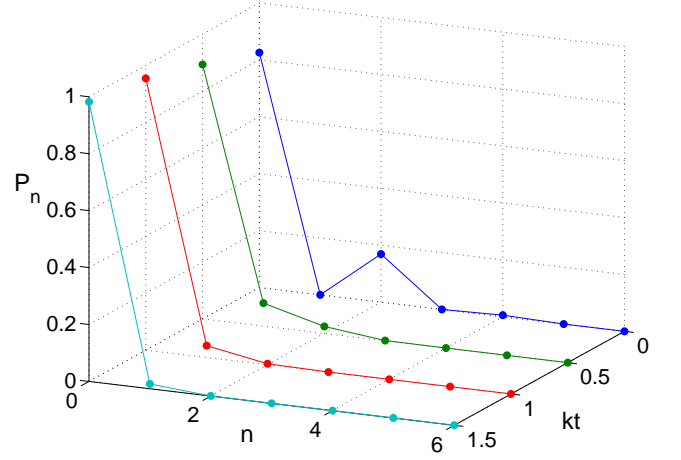


FIG. 8: Time evolution of the photon number distribution for an even superposition state ($\theta = 0$). Parameters: $\beta_0 = 0.8$, $\omega = 1$, $k = 0.1$.

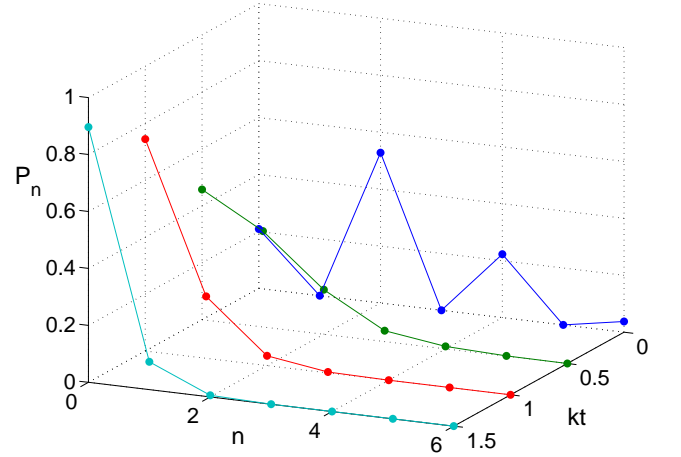


FIG. 9: Time evolution of the photon number distribution for an even superposition state ($\theta = 0$). Parameters: $\beta_0 = 1.5$, $\omega = 1$, $k = 0.1$.

and for the superposition states considered

$$S[\rho_A] = -p_o \ln p_o - p_e \ln p_e. \quad (21)$$

Note that the entropy increases up to the decoherence time, when it starts decreasing back to zero, which is the entropy of the asymptotic state of the dissipative reservoir, the vacuum. The shape of the curve changes for large values of β_0 and the decoherence time is smaller, as expected.

III. GAUSSIAN STATES: DISPLACED, SQUEEZED, THERMAL STATES (GSS)

We start with the Liouvillian given in Eq. (4), but now we extend the calculations in order to include

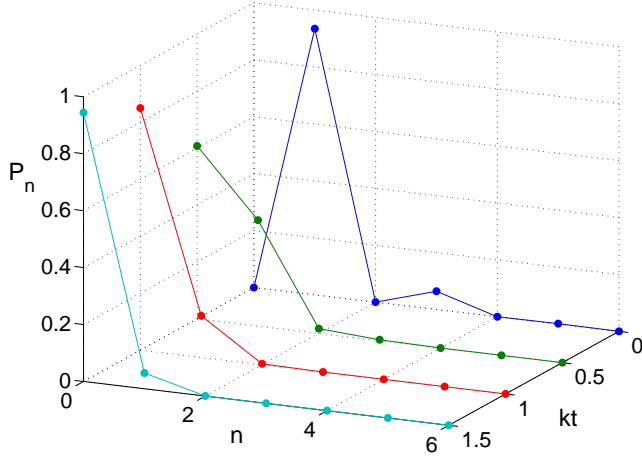


FIG. 10: Time evolution of the photon number distribution for an odd superposition state ($\theta = \pi$). Parameters: $\beta_0 = 0.8$, $\omega = 1$, $k = 0.1$.

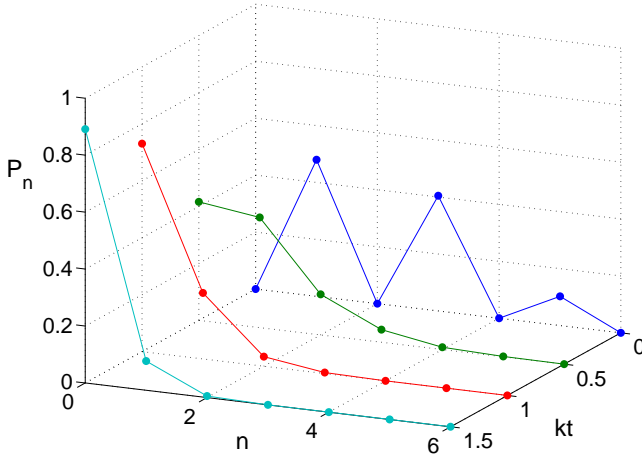


FIG. 11: Time evolution of the photon number distribution for an odd superposition state ($\theta = \pi$). Parameters: $\beta_0 = 1.5$, $\omega = 1$, $k = 0.1$.

temperature, i.e., we consider $\bar{n}_B \geq 0$.

If the initial state is a Gaussian, it can be written as

$$\rho_B = \mathcal{D}(\alpha_0) \mathcal{S}(r_0, \phi_0) \rho_{\nu_0} \mathcal{S}^\dagger(r_0, \phi_0) \mathcal{D}^\dagger(\alpha_0) \quad (22)$$

where $\mathcal{D}(\alpha)$ is the displacement operator, $\mathcal{S}(r, \phi)$ is the squeezing operator, the subscript 0 denotes initial values and ρ_ν is the thermal density operator with average number of excitations ν . More explicitly we have

$$\mathcal{D}(\alpha) = \exp(\alpha a^\dagger - \alpha^* a) \quad (23)$$

$$\mathcal{S}(r, \phi) = \exp\left(\frac{1}{2} r e^{i\phi} a^{\dagger 2} - \frac{1}{2} r e^{-i\phi} a^2\right) \quad (24)$$

$$\rho_\nu = \frac{1}{1+\nu} \exp\left[\ln\left(\frac{\nu}{\nu+1}\right) a^\dagger a\right] \quad (25)$$

We remark that ν is *not* the average number of excita-

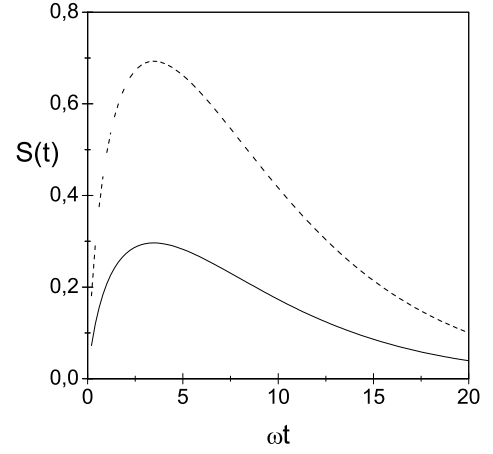


FIG. 12: von Neumann's entropy for the even superposition state ($\theta = 0$, solid line) and for the odd superposition state ($\theta = \pi$, dash line). Parameters: $\beta_0 = 0.8$, $\omega = 1$, $k = 0.1$.

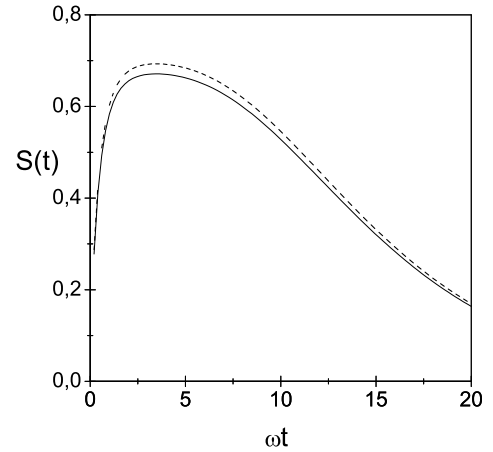


FIG. 13: von Neumann's entropy for the even superposition state ($\theta = 0$, solid line) and for the odd superposition state ($\theta = \pi$, dash line). Parameters: $\beta_0 = 1.5$, $\omega = 1$, $k = 0.1$.

tions, but rather the average number of *thermal* excitations. The evolution preserves the Gaussian character of the density operator, and the parameters acquire a time dependence, i. e., the state becomes

$$\rho_B = \mathcal{D}(\alpha) \mathcal{S}(r, \phi) \rho_\nu \mathcal{S}^\dagger(r, \phi) \mathcal{D}^\dagger(\alpha) \quad (26)$$

where

$$\alpha(t) = \alpha_0 e^{-(i\omega+k)t} \quad (27)$$

$$\phi(t) = \phi_0 - 2\omega t \quad (28)$$

$$\nu(t) = \sqrt{x^2(t) - \left[\left(\nu_0 + \frac{1}{2} \right) \sinh(2r_0) e^{-2kt} \right]^2} - \frac{1}{2} \quad (29)$$

$$x(t) = \left(\nu_0 + \frac{1}{2} \right) \cosh(2r_0) e^{-2kt} + \left(\bar{n}_B + \frac{1}{2} \right) (1 - e^{-2kt}) \quad (30)$$

$$r(t) = \frac{1}{4} \ln \left[\frac{(\nu_0 + \frac{1}{2}) e^{2r_0} + (\bar{n}_B + \frac{1}{2}) (e^{2kt} - 1)}{(\nu_0 + \frac{1}{2}) e^{-2r_0} + (\bar{n}_B + \frac{1}{2}) (e^{2kt} - 1)} \right] \quad (31)$$

The Robertson-Schroedinger determinant (or the covariance matrix) and the von Neumann entropy are related by

$$D(t) = \left[\nu(t) + \frac{1}{2} \right]^2 \quad (32)$$

$$S[\rho(t)] = [\nu(t) + 1] \ln [\nu(t) + 1] - \nu(t) \ln \nu(t). \quad (33)$$

Note that, in the case of Gaussian states, the entropy is completely determined by a relationship between quadratures, given by $D(t)$, and is always analytical. Note also that, differently from the superposition states, the entropy is independent of the optical field intensity, which may turn on an experimental advantage. Here, optical field intensity means the displacement.

A. Squeezing

The Wigner function of the GSS is always positive. The evolved Wigner function for a GSS described by the Liouvillian (4) acting on the Gaussian initial state (22) is

$$\begin{aligned} W(q, p) = & \sum_l \frac{1}{\pi} \frac{(-|F_3| \nu)^l}{(\nu + 1)^{l+1}} \\ & \times L_l \left[2 \left(\frac{(x - x_0)^2}{F_4^2} + \frac{(F_4 F_5)^2}{4} \right) \right] \\ & \times \frac{F_4}{|F_1|} \exp \left[-\frac{(x - x_0)^2}{F_4^2} - \frac{(F_4 F_5)^2}{4} \right], \end{aligned} \quad (34)$$

where $L_l(x)$ is the Laguerre function of l order and argument x and we define [24]

$$\begin{aligned} F_1 &= \cosh r + e^{i\phi} \sinh r, \\ F_2 &= \frac{1 - i \sin \phi \sinh r (\cosh r + e^{i\phi} \sinh r)}{(\cosh r + \cos \phi \sinh r) (\cosh r + e^{i\phi} \sinh r)}, \\ F_3 &= \frac{\cosh r + e^{-i\phi} \sin \phi \sinh r}{\cosh r + e^{i\phi} \sin \phi \sinh r}, \\ F_4 &= \sqrt{\cosh^2 r + \sinh^2 r + 2 \cos \phi \cosh r \sinh r}, \\ F_5 &= 2(p + p_0) - i(x - x_0)(F_2^* - F_2). \end{aligned} \quad (35)$$

The time evolution of the parameters are given by Eq. (27)-(31).

We can access the squeezing by looking at the determinant of the covariance matrix (32) (and consequently looking at the entropy (33)). In figure (14) we show the determinant of the covariance matrix versus time. Its behavior (and the discussion) is very similar to the one of the even superposition state showed before. Here, the time of the maximum value of the determinant is (this result was also found in ref. [25], for the linear entropy)

$$\begin{aligned} t_c^G &= (2k)^{-1} \left\{ \ln 2 - \ln \left[\frac{2\bar{n}_B + 1}{d} \right. \right. \\ &\quad \times \left. \left. (2\nu_0 \cosh(2r_0) + \cosh(2r_0) - 2\bar{n}_B - 1) \right] \right\} \end{aligned} \quad (36)$$

where

$$\begin{aligned} d &= 2 \cosh(2r_0) \left[\bar{n}_B (\nu_0 + 1) + \nu_0 (\bar{n}_B + 1) + \frac{1}{2} \right] \\ &\quad - 2 \left(\bar{n}_B + \frac{1}{2} \right)^2 - 2 \left(\nu_0 + \frac{1}{2} \right)^2. \end{aligned}$$

We remark that we assume the characteristic time to be positive, i. e. if $t_c^G > 0 \longrightarrow t_c^G \in \mathbb{R}$. The “quantum properties” present in the state are visible for ν_0 satisfying [20]

$$\nu_0 < \frac{1}{2} [2\bar{n}_B \cosh(2r_0) + \cosh(2r_0) - 1]. \quad (37)$$

Of course, this visibility is also a consequence of two factors: the initial conditions need to obey the above inequality (37) and the time scale (36) needs to be experimentally accessible.

Equation (37) establishes an upper bound on the initial “impurity” of the state such that, even under a dissipative environment, squeezing can be accessed.

It is rather remarkable that this characteristic time is independent of the field intensity. This has been shown numerically in reference [19]. For our choice of parameters, t_c^G is comparable to t_c^S (superposition time scale). However, it is possible to obtain $t_c^G \gg t_c^S$, e.g., by simply increasing the field intensity of the coherent superposition state. As an example, if we impose $\langle a^\dagger a \rangle_{GSS} = \langle a^\dagger a \rangle_{CSS}$ and choose the following parameters: $\omega = 1$, $n_B = 0$, $k = 0.1$, $\nu_0 = 0$, $|\beta_0| = 0.8$, $\alpha_0 = 0.0$

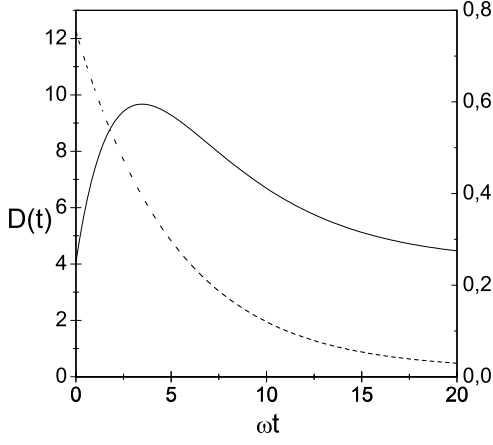


FIG. 14: Time evolution of the determinant of the covariance matrix for the GSS. Parameters: $\omega = 1$, $n_B = 0$, $k = 0.1$, $r_0 = 1$, $\nu_0 = 0$ (solid line, right scale) and $\nu_0 = 3$ (dashed line, left scale).

and $\theta = 0$, the squeezing factor must be $r_0 \simeq 0.73$ and the characteristic times will respect

$$0 < t_c^S < t_c^G < \tau, \quad (38)$$

where τ is the decoherence time for the CSS, t_c^S and t_c^G is given by (15) and (36) respectively.

B. Oscillating photon distribution

Analyzing the displaced squeezed Gaussian states, one can see that they also have super-Poissonian statistic (as the even superposition state). This is measured by the Mandel parameter: for a GSS with the dynamics given by (4) we always have $Q \geq 0$. For a GSS it is known that the photon distribution is (given in [25, 26])

$$\begin{aligned} P_n &= \pi Q(0) (-1)^n 2^{-2n} (\tilde{A} + |\tilde{B}|)^n \\ &\times \sum_{k=0}^n \frac{1}{k!(n-k)!} \left[\frac{\tilde{A} - |\tilde{B}|}{\tilde{A} + |\tilde{B}|} \right]^k \\ &\times H_{2k} \left[i \frac{\Im(\tilde{C} e^{-i\frac{\phi}{2}})}{\sqrt{\tilde{A} - |\tilde{B}|}} \right] \\ &\times H_{2n-2k} \left[i \frac{\Re(\tilde{C} e^{-i\frac{\phi}{2}})}{\sqrt{\tilde{A} + |\tilde{B}|}} \right] \end{aligned} \quad (39)$$

where H_j is the j -order Hermite polynomial and

$$\begin{aligned} \pi Q(0) &= [(1+A)^2 - |B|^2]^{1/2} \\ &\times \exp \left\{ - \frac{(1+A)|C|^2 + \frac{1}{2}[B(C^*)^2 + B^*C^2]}{(1+A)^2 - |B|^2} \right\} \end{aligned} \quad (40)$$

where

$$A = \nu + (2\nu + 1) \sinh^2 r \quad (41)$$

$$B = -(2\nu + 1) e^{i\phi} \sinh r \cosh r \quad (42)$$

$$C = \alpha \quad (43)$$

and finally

$$\tilde{A} = \frac{\nu(\nu + 1)}{\nu^2 + (\nu + \frac{1}{2})[1 + \cosh(2r)]} \quad (44)$$

$$\tilde{B} = - \frac{e^{i\phi}(\nu + \frac{1}{2}) \sinh(2r)}{\nu^2 + (\nu + \frac{1}{2})[1 + \cosh(2r)]} \quad (45)$$

$$\tilde{C} = \frac{C[\frac{1}{2} + (\nu + 1/2) \cosh(2r)] - C^* e^{i\phi}(\nu + \frac{1}{2}) \sinh(2r)}{\nu^2 + (\nu + \frac{1}{2})[1 + \cosh(2r)]}. \quad (46)$$

The time evolution of P_n is presented in figures (15)-(16). It is clear that, if the states respect (37) oscillations in the photon distribution are observable, else the photon distribution look like a “thermal” one.

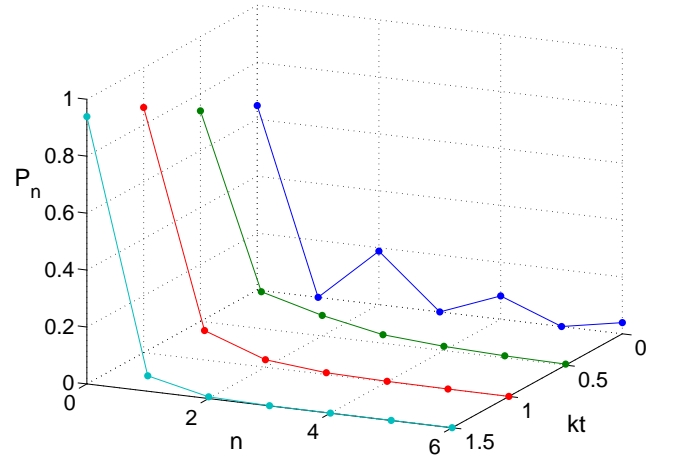


FIG. 15: Photon number distribution for a GSS with $\alpha_0 = 0$, $\phi_0 = 0$, $r_0 = 1$, $k = 0.1$, $\nu_0 = 0$ and $\bar{n}_B = 0$.

Following the idea of [27] the second order correlation function for Gaussian Squeezed States (GSS) is a “quantum witness”

$$g^{(2)}(0) = \frac{\langle a^\dagger a^\dagger a a \rangle}{\langle a^\dagger a \rangle^2}. \quad (47)$$

If $g^{(2)} > 3$ the GSS is quantum, if $g^{(2)} \leq 3$ the state is classical. We see that for values respecting (37) the state is quantum according this criterion. The Mandel parameter Q for a GSS shows, like the even superposition state, super-Poissonian statistic $Q > 0$, and when $t \rightarrow \infty$ the statistic tends to Poissonian.

C. von Neumann entropy

In a recent work [20] we studied some characteristics of the GSS, including photon number distribution, Wigner

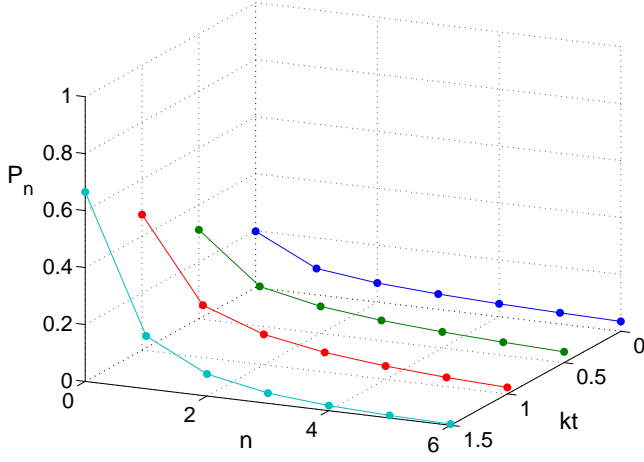


FIG. 16: Photon number distribution for a GSS with $\alpha_0 = 0$, $\phi_0 = 0$, $r_0 = 1$, $k = 0.1$, $\nu_0 = 3$ and $\bar{n}_B = 0$.

function and von Neumann entropy. We show the results here for the purpose of comparison with the superposition states (similar behaviour was found also in [16], where they studied the 2-entropy of a single-mode field initially in a number state). In figure (17) we show the result for the von Neumann entropy for the GSS, for different values of ν_0 . The characteristic time for the entropy is the same, in this case, as the characteristic time for squeezing, and we can conclude that the same condition (i. e., equation (37)) holds here too. Note also that the entropy (and any other observable that depends only on $\nu(t)$) is *independent* of the field strength $\alpha(t)$ and the squeezing phase $\phi(t)$.

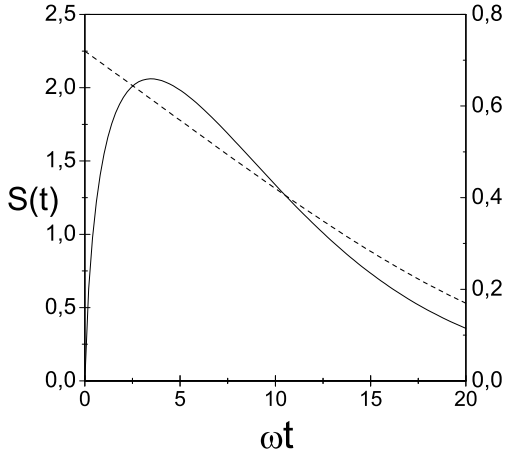


FIG. 17: Time evolution of the determinant of the von Neumann entropy for the GSS. Parameters: $\omega = 1$, $n_B = 0$, $k = 0.1$, $r_0 = 1$, $\nu_0 = 0$ (solid line, right scale) and $\nu_0 = 3$ (dashed line, left scale).

IV. GSS VERSUS SUPERPOSITION STATES – FIDELITY

In the previous sections we briefly review some properties of coherent superposition states and of GSS, and how these properties evolve in time. We compare these states by graphically analyzing the evolution of those properties and, although qualitatively, we could get some conclusions and made some comparisons between the studied states.

Now we present a more quantitative comparison between the states, through the fidelity, defined by

$$F = \text{tr} \sqrt{\sqrt{\rho_A} \rho_B \sqrt{\rho_A}} \quad (48)$$

where ρ_A and ρ_B are (5) and (26) respectively. With this result we can quantify how the states “look like” each other.

The expression for the fidelity is

$$F = \sqrt{\lambda_+} + \sqrt{\lambda_-}, \quad (49)$$

where

$$\lambda_{\pm} = \frac{b + c \pm \sqrt{(b - c)^2 + 4|d|^2}}{2} \quad (50)$$

and

$$\begin{aligned} b &= p_e \langle e | \rho_B | e \rangle \\ &= \frac{p_e}{N_e^2} \left\{ \langle \beta | \rho_B | \beta \rangle + \langle -\beta | \rho_B | -\beta \rangle + 2\Re \langle -\beta | \rho_B | \beta \rangle \right\} \end{aligned} \quad (51)$$

$$\begin{aligned} c &= p_o \langle o | \rho_B | o \rangle \\ &= \frac{p_o}{N_o^2} \left\{ \langle \beta | \rho_B | \beta \rangle + \langle -\beta | \rho_B | -\beta \rangle - 2\Re \langle -\beta | \rho_B | \beta \rangle \right\} \end{aligned} \quad (52)$$

$$\begin{aligned} d &= \sqrt{p_e p_o} \langle e | \rho_B | o \rangle \\ &= \frac{\sqrt{p_e p_o}}{N_e N_o} \left\{ \langle \beta | \rho_B | \beta \rangle - \langle -\beta | \rho_B | -\beta \rangle + 2i\Im \langle -\beta | \rho_B | \beta \rangle \right\}. \end{aligned} \quad (53)$$

The other terms are

$$\begin{aligned} \langle \beta | \rho_B | \beta \rangle &= \frac{1}{\sqrt{(\nu + 1)^2 \cosh^2 r - \nu^2 \tanh^2 r}} \\ &\times \exp \left\{ \frac{(2\nu + 1) \tanh r \Re[\eta^2]}{(\nu + 1)^2 - \nu^2 \tanh^2 r} \right\} \\ &\times \exp \left\{ -\frac{|\eta|^2 [(\nu + 1) + \nu \tanh^2 r]}{(\nu + 1)^2 - \nu^2 \tanh^2 r} \right\} \end{aligned} \quad (54)$$

$$\begin{aligned}
\langle -\beta | \rho_B | -\beta \rangle &= \frac{1}{\sqrt{(\nu+1)^2 \cosh^2 r - \nu^2 \tanh^2 r}} \\
&\times \exp \left\{ \frac{(2\nu+1) \tanh r \Re[\zeta^2]}{(\nu+1)^2 - \nu^2 \tanh^2 r} \right\} \\
&\times \exp \left\{ -\frac{|\zeta|^2 [(\nu+1) + \nu \tanh^2 r]}{(\nu+1)^2 - \nu^2 \tanh^2 r} \right\}
\end{aligned} \tag{55}$$

$$\begin{aligned}
\langle -\beta | \rho_B | \beta \rangle &= \frac{1}{\sqrt{(\nu+1)^2 \cosh^2 r - \nu^2 \tanh^2 r}} \\
&\times \exp \left\{ \frac{(2\nu+1) \tanh r [\zeta^2 + \eta^2]}{2(\nu+1)^2 - 2\nu^2 \tanh^2 r} \right\} \\
&\times \exp \left\{ -\frac{|\zeta|^2 + |\eta|^2}{2} \right. \\
&\quad \left. - \frac{\zeta \eta \nu (\nu+1)}{(\nu+1)^2 \cosh^2 r - \nu^2 \sinh^2 r} \right\}
\end{aligned} \tag{56}$$

where we define

$$\zeta = (\beta^* + \alpha^*) e^{i\frac{\phi}{2}} \tag{57}$$

$$\eta = (\beta - \alpha) e^{-i\frac{\phi}{2}}. \tag{58}$$

To understand the (big and cumbersome) expressions for the fidelity we plot the fidelity against time in figures (18) - (21) (the time scale of the graphics is: time = ωt). The choice $\alpha_0 \simeq 0.0$ is due to numeric computations. In fact we use $\alpha_0 = 10^{-20}$. In each figure, we show the decoherence time τ for the CSS, *i.e.* $\tau = (4|\beta_0|^2 k)^{-1}$ and the squeezing characteristic time for CSS and for GSS - (15) and (36) in the vertical lines.

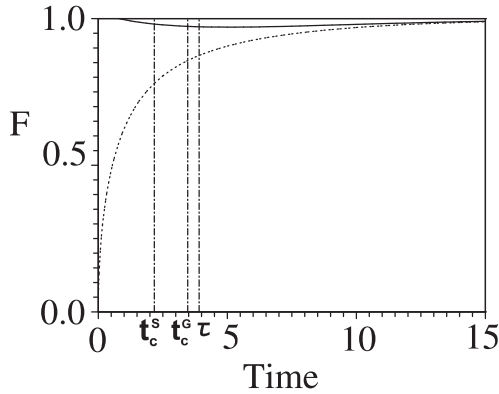


FIG. 18: Fidelity between the coherent superposition states and the GSS. The parameters used: $\beta_0 = 0.8$, $w = 1$, $k = 1$, $r_0 = 1$, $\alpha_0 \simeq 0.0$, $\phi_0 = 0$, $n_B = 0$, $\nu_0 = 0$, $\theta = 0$ (solid line) and $\theta = \pi$ (dash line). The initial value of F for the even CSS is greater than 1 due to limitations in the numeric routine used.

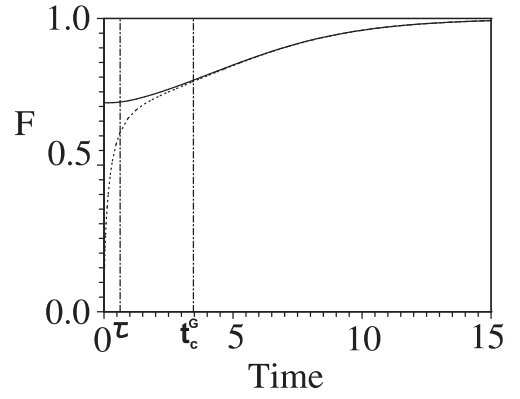


FIG. 19: Fidelity between the coherent superposition states and the GSS. The parameters used: $\beta_0 = 2.0$, $w = 1$, $k = 1$, $r_0 = 1$, $\alpha_0 \simeq 0.0$, $\phi_0 = 0$, $n_B = 0$, $\nu_0 = 0$, $\theta = 0$ (solid line) and $\theta = \pi$ (dash line).

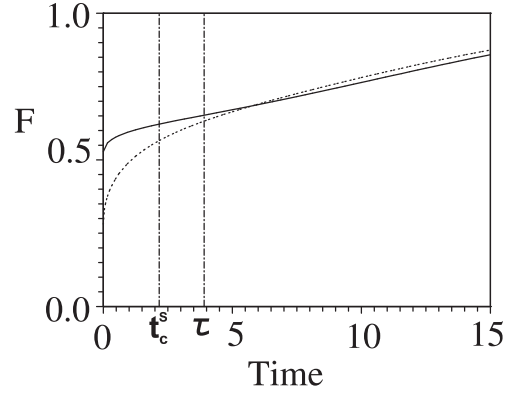


FIG. 20: Fidelity between the coherent superposition states and the GSS. The parameters used: $\beta_0 = 0.8$, $w = 1$, $k = 1$, $r_0 = 1$, $\alpha_0 \simeq 0.0$, $\phi_0 = 0$, $n_B = 0$, $\nu_0 = 3$, $\theta = 0$ (dash line) and $\theta = \pi$ (solid line).

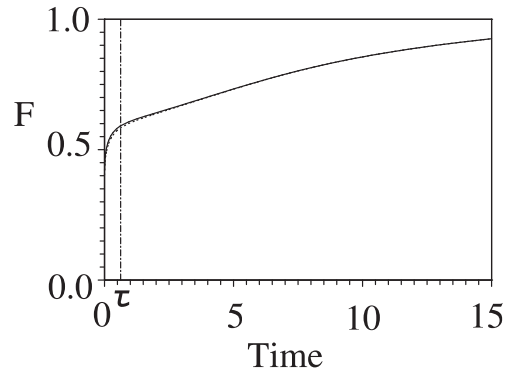


FIG. 21: Fidelity between the coherent superposition states and the GSS. The parameters used: $\beta_0 = 2.0$, $w = 1$, $k = 1$, $r_0 = 1$, $\alpha_0 \simeq 0.0$, $\phi_0 = 0$, $n_B = 0$, $\nu_0 = 3$, $\theta = 0$ (dash line) and $\theta = \pi$ (solid line).

Analyzing the figures we can conclude the same as we did before, but in a more quantitative way. In figures (18) and (19) we plot the fidelity between a squeezed Gaussian state with $\nu_0 = 0$ and even and odd superposition states with $\beta_0 = 0.8$ and $\beta_0 = 2.0$, respectively. One can see that the initial fidelity is always high for the even superposition state with short values of β_0 , while when we increase this parameter the fidelity decreases. The even superposition with $\beta_0 = 0.8$ is approximately a Gaussian state - apart the fact that it has negative Wigner function - and it behaves like the GSS, i. e., the squeezing property dominates the other quantum ones. When we increase β_0 , the interference property dominates and the state does not resemble the GSS. For values of β_0 not respecting the inequality (16) we see that the even superposition state does not possess high fidelity and rapidly behaves like the odd one.

In figures (20) and (21) we show the results for the GSS with $\nu_0 = 3$ and even and odd superposition states with $\beta_0 = 0.8$ and $\beta_0 = 2.0$, respectively. Both the even and the odd superposition states behave similarly in these cases. In the first case the GSS is not “so squeezed” as the even superposition state and the fidelity between them is short. In the second case, the interference property dominates the superposition states and their fidelity against the GSS behaves practically equal.

V. SUMMARY AND CONCLUSIONS

In this work we study in detail, quantum properties of coherent superposition states (even and odd superposi-

tion states) and of displaced, squeezed, thermal states. We analyze the squeezing (via the Wigner function and the covariance matrix determinant), the oscillations in photon distribution (through the diagonal term of the density operator $\rho_{nn} = P_n$) and the von Neumann entropy ($S[\rho] = -\text{tr}[\rho \ln \rho]$) for both cases. We show that in superposition states each property has different characteristic time (being the “squeeze time” lesser than the decoherence time) while in the GSS we found only one characteristic time (36). The even superposition state shows squeezing, just like the GSS, and we can access this property via the covariance matrix. We show that, for both cases (even superposition state and GSS) the squeezing effect only can be observed in special initial conditions - equations (16) and (37) - and in experimentally accessible time scales - (15) and (36). Since it is “easy” to observe quadratures (for example with homodyne detection), one can use the squeezing effect to study quantum information, provided the initial conditions fulfill the inequalities cited before. Finally, we compare these effects more quantitatively by analyzing the fidelity between the GSS and the superposition states (even and odd), concluding the same, i. e., if the states respect the inequalities mentioned before (the GSS and the even superposition state for instance), the fidelity has high value.

Acknowledgments. The authors thank funding from Brazilian agencies CNPq and FAPEMIG.

-
- [1] S. L. Braustein and A. K. Pati, *Quantum information with continuous variables*. Kluwer Academic, Dordrecht (2003); S. L. Braunstein and P. van Loock, Rev. Mod. Phys. **77**, 513 (2005).
 - [2] H. A. Bachor, *A guide to experiments in quantum optics*. (John Wiley & Sons, 1988).
 - [3] M. S. Kim, F. A. M. de Oliveira, and P. L. Knight, Phys. Rev. A **40**, 2494 (1989).
 - [4] K. Wódkiewicz et al, Phys. Rev. A **35**, 2567 (1987).
 - [5] L. Mandel, Phys. Scr. **T12**, 34 (1986).
 - [6] P. Adam and J. Janszky, Phys. Lett. A **149**, 67 (1990).
 - [7] V. Bužek and P. L. Knight, Opt. Comm. **81**, 331 (1991).
 - [8] A. Vidiella-Barranco et al, in *Quantum measurement in Optics*. NATO Advanced Study Institute, ed. by P. Tombesi and D. F. Walls (Plenum, N.Y. 1991).
 - [9] V. Bužek, A. Vidiella-Barranco and P. L. Knight, Phys. Rev. A **45**, 6570 (1992).
 - [10] V. Bužek, P. L. Knight and A. Vidiella-Barranco, in *Squeezing and Uncertainty Relations*, ed. by D. Han and Y. S. Kim (NASA, Washington DC, 1991).
 - [11] W. Schleich, M. Pernigo and F. L. Kien, Phys. Rev. A **44**, 2172 (1991).
 - [12] C. K. Hong and L. Mandel, Phys. Rev. Lett. **54**, 323 (1985).
 - [13] L. Mandel, Opt. Lett. **4**, 205 (1979); see also Phys. Scr. **T12**, 34 (1986).
 - [14] B. Yurke and D. Stoler, Phys. Rev. Lett. **57**, 13 (1986).
 - [15] P. Marian and T. A. Marian, J. Phys. A: Math. Gen. **33**, 3595 (2000).
 - [16] P. Marian and T. A. Marian, Eur. Phys. J. D **11**, 257 (2000).
 - [17] L. Mandel, Opt. Lett. **4**, 205 (1979).
 - [18] A. Serafini, M. G. A. Paris, F. Illuminati and S. De Siena, J. Opt. B: Quantum Semiclass. Opt. **7**, R19-R36 (2005). Gerardo Adesso and Fabrizio Illuminati, J. Phys. A: Math. Theor. **40**, 78217880 (2007). A. Serafini, F. Illuminati, M. G. A. Paris, S. De Siena, Phys. Rev. A **69**, 022318 (2004).
 - [19] M. G. A. Paris, F. Illuminati, A. Serafini and S. De Siena, Phys. Rev. A **68**, 012314 (2003).
 - [20] L. A. M. Souza and M. C. Nemes, arXiv:0706.4271v1 [quant-ph].
 - [21] M. Brune, S. Haroche, J. M. Raimond, L. Davidovich, and N. Zagury, Phys. Rev. A **45**, 5193 (1992); L. Davidovich, M. Brune, J. M. Raimond, and S. Haroche, ibid. **53**, 1295 (1996).
 - [22] B. Wang and L.-M. Duan, Phys. Rev. A **72**, 022320 (2005); Zhi-Ming Zhang, Ashfaq H Khosa, Manzoor

- Ikram and M Suhail Zubairy, J. Phys. B: At. Mol. Opt. Phys. **40** 1917 (2007).
- [23] K. M. Fonseca Romero, M. C. Nemes, J. G. Peixoto de Faria, A. N. Salgueiro and A. F. R. de Toledo Piza, Phys. Rev. A **58**, 3205 - 3209 (1998).
- [24] M. M. Nieto, Phys. Lett. A **229**, 135 (1997).
- [25] P. Marian and T. A. Marian, Phys. Rev. A **47**, 4487 (1993).
- [26] P. Marian and T. A. Marian, Phys. Rev. A **47**, 4474 (1993).
- [27] Magdalena Stobinska and Krzysztof Wodkiewicz, Phys. Rev. A **71**, 032304 (2005).